Alexandria Engineering Journal (2016) 55, 2621–2630

HOSTED BY

Alexandria University

Alexandria Engineering Journal

www.elsevier.com/locate/aej
www.sciencedirect.com

SHORT COMMUNICATION

Design and characterization of a tunable patch antenna loaded with capacitive MEMS switch using CSRRs structure on the patch

Rajesh Saha, Santanu Maity *, Chandan Tilak Bhunia

Electronics and Communication Engineering, National Institute of Technology, Arunachal Pradesh, India

Received 31 October 2015; revised 23 March 2016; accepted 4 May 2016
Available online 24 May 2016

KEYWORDS

Tunable;
RF-MEMS switch;
Micromachining;
CPW

Abstract In this paper, the design and characterization of a tunable patch antenna loaded with complementary split ring resonators (CSRRs) on the patch have been realized. To achieve tunable resonant frequency, bandwidth and radiation pattern, the antenna is further loaded with coplanar waveguide (CPW) on which Microelectromechanical System (MEMS) capacitive switches are placed periodically. The tunable property is achieved, when the switches moves from up state with the capacitive gap 1.5 μm to down state having capacitive gap of 1 μm. A parametric analysis has been presented to check the sensitivity of the antenna in terms of S11 parameter by varying different parameters of the MEMS switches and CSRRs. This work, strives to improve the degree of reconfigurability with increase in the number of switches. The value of actuation voltage to move switch from up to down state is 10.4 V, which is very low over the other design. The switches exhibit fundamental frequency 14.6 kHz, switching time 28.59 μs, and capacitance ratio 15.27. Simulation has been carried out in Ansoft HFSS v. 13 and the distinct characterization property of the tunable antenna is shown through simulation.

1. Introduction

Nowadays, different antennas are required to be designed for different applications in achieving better performance in wireless communication. The performance achieved by the antennas is very significant for any communication system. However, by introducing Radio Frequency Microelectromechanical Systems (RF-MEMS) switch technology, a single antenna can be tuned at different resonant frequency, bandwidth, and radiation pattern; and hence may be applied to distinct applications [1]. Since 1970, MEMS technology has been developed for pressure and temperature sensors, accelerometers, and other sensor devices [2]. Recent advancement in MEMS technology was extremely beneficial to military and commercial applications, and from the last few decades their application has spread in fields such as satellite communication, wireless communication and air traffic control [3,4]. In MEMS technology, the mechanical portion is monolithically integrated with the electrical component. MEMS device and circuit have been fabricated on the same silicon chip by using

* Corresponding author.
E-mail addresses: rajeshsaha93@gmail.com (R. Saha), santanu.ece@nitap.in (S. Maity).
Peer review under responsibility of Faculty of Engineering, Alexandria University.

http://dx.doi.org/10.1016/j.aej.2016.05.002

micro fabrication. MEMS device can offer attractive features in comparison with solid-state device (e.g., semiconductor switches, varactor diodes, PIN diode), such as very low loss, wide operating frequency band, lower signal attenuation, and higher level of isolation [5]. If RF-MEMS component can replace traditional devices in wireless communication then the system becomes very compact in size and will consume very less power. The application of MEMS switch to RF system has given birth to tunable components with better performance in terms of lower power consumption, high reliability, linearity, isolation, and compatibility with integrated circuit [6,7]. The tunability property is also known as reconfigurable characteristic. Reconfigurability of an antenna can be achieved by altering radiation pattern, polarization, and bandwidth with marginally changing its physical structure [8]. In most literatures, we have found only one single switch is used throughout the system. However, for any application needs of maximum reconfigurability [9], the use of single switch is not sufficient. The level of reconfigurability can be enhanced by utilizing multiple switch membrane on CPW.

In this paper, a tunable antenna loaded with CSRRs structure on the patch was presented. The tunable in frequency, bandwidth, and radiation pattern is achieved by loading the antenna CPW on which RF-MEMS capacitive switches are placed. This paper also demonstrates how maximum reconfigurability can be achieved by increasing the number of switches in parallel connection on the CPW. The analytical value of actuation voltage to reach the down state of MEMS switch from the up state and switching time of each beam has also been estimated in the paper. The proposed model has very low actuation voltage. An elaborate discussion on the proposed device structures is shown in Section 2. Mechanical and electrical properties of MEMS switched capacitors are also discussed in Section 3. Results and discussion of the proposed model have been shown in Section 4. Section 5 gives the parametric analysis in terms of S11 parameters for MEMS switches and CSRRs. Lastly, Section 6 concludes the work.

2. Device structures

The proposed antenna with Cartesian co-ordinate system is shown in Fig. 1. Initially, a rectangular patch antenna has been designed on high dielectric constant (ε_r = 11.9) silicon substrate having substrate thickness of 275 μm. The patch and ground are made of gold. The antenna designed on silicon provides compatibility with CMOS technology and is also cost effective in terms of fabrication and packaging. Microstrip patch antenna has bandwidth in the order of 1–5%. This bandwidth can be enhanced ether by decreasing dielectric constant or by increasing height of the substrate thickness. Hence, if Si is used as a substrate [10] which has very high permittivity value (11.9) then the bandwidth of patch antenna decreases and excitation of surface wave increases. Hence it results in degradation in gain and efficiency of the antenna.

In order to overcome these problems an air cavity has been created between the patch and the ground, through the process called bulk micromachining [11,12]. By using micromachining the effective permittivity value decreases but the size of antenna slightly increases compared to antenna on pure silicon substrate. Papapolymerou and Drayton [13] proposed a mathematical equation to calculate the effective permittivity value within the cavity with respect to air. Eq. (1) gives the accurate result to calculate the effective value of permittivity (ε_{cavity}) within the air cavity with respect to substrate.

$$\varepsilon_{cavity} = \frac{\varepsilon_{Si}\varepsilon_{air}}{\varepsilon_{air} + (\varepsilon_{Si} - \varepsilon_{air})x_{air}} \tag{1}$$

where ε_{Si}, ε_{air} and x_{air} are the permittivity of silicon substrate, the permittivity of air, and ratio of air cavity height to full substrate thickness respectively. In proposed designed, an air cavity of height 225 μm was created and after calculating the value of permittivity (ε_{cavity}) within the cavity is 1.197. The micromachining part of MEMS antenna is shown in Fig. 2. In consecutive step, in order to further improve the performance of the antenna, a structure of CSRRs has been loaded on the patch. The dimension of each CSRR has been shown in Fig. 1 and feeding technique used to excite the antenna is inset feeding method. The slots on the patch: to end of the feed line, near signal line of CPW and opposite side of feeding line were created for achieving the proper impedance matching.

In next step, the antenna is loaded with CPW stub on which MEMS shunt switches are placed periodically at 0.2 mm distance. The dimension of each switch is 2.08 mm × 0.2 mm. In order to make the antenna tunable in frequency, the height of the bridges on the CPW stub has to be changed; hence, loading capacitors can be changed by applying dc actuation voltage between the center conductor and the MEMS bridges.

Fig. 1 portrays top view of tunable antenna loaded with four switches. First, the simulation by activating one switch only has done. But in some applications we need antenna with very high level reconfigurability. Finally, to increase the level of reconfigurability increase the number of active switches loaded in parallel on the CPW. More switches, can contribute to larger capacitance value and results in increase in margin of reconfigurability.

3. RF MEMS switch and its properties

3.1. MEMS switch

Fig. 1 represents the integration of MEMS switch with patch antenna on same silicon substrate to achieve tunable in performance. MEMS switch may be series or shunt type depending on signal path and it can also be electrostatic, magnetostatic depending on the actuation mechanism [14]. In our designed, we have chosen shunt switch over series, as it involves minimum parasitic elements and also handles more power compared to series switch. The switch is a metal bridge suspended over the center conductor of CPW and fixed both ends of the bridge to ground of CPW. A thin dielectric layer of silicon nitride, which works as an insulator is deposited above the center line of CPW. The bridge can be moved from up to down state by applying the bias voltage between the MEMS bridges and CPW center conductor [15,16]. At up state, an air gap is present between the dielectric layer and bridge; hence by reducing this capacitive gap, the tunability in frequency can be obtained. When an actuation dc voltage is applied between the bridge of the switch and CPW signal line, the switch goes to down from the up state and hence the resonance frequency is changed from the previous up state value. The figure of merit of MEMS switch depends upon the capacitance ratio (C_r) of down to up state (C_{down}/C_{up}), which

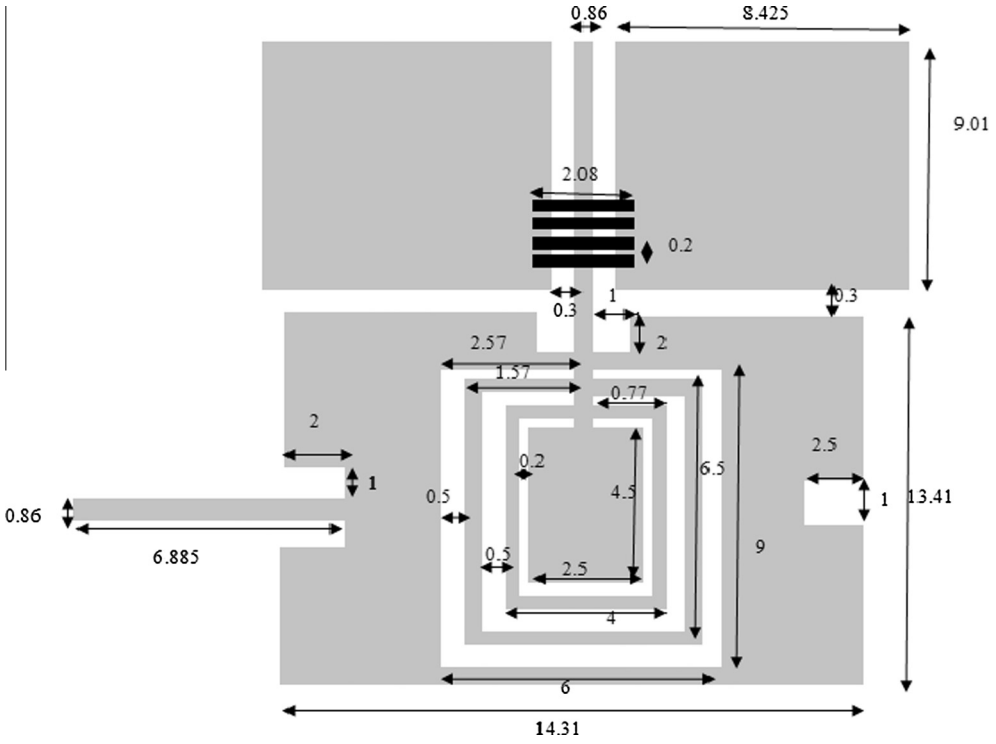

Figure 1 Top view of tunable antenna loaded with four MEMS switches (dimensions are in mm).

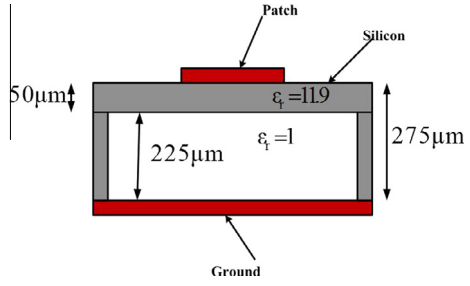

Figure 2 View of micromachining part of the antenna.

primarily dependent on dimension of the switch [17,18]. Pictorial views of MEMS switch with fixed–fixed beam are shown in Fig. 3. In Fig. 3, F_e and F are the electrostatic and magneto static force respectively; l, t and w are the length, thickness and width of the beam respectively. W and t_d are width of the central line of CPW and thickness of isolation layer respectively. L is the length of the beam excluding the length of two anchors and g_0 is the initial gap between the central line of CPW and the beam.

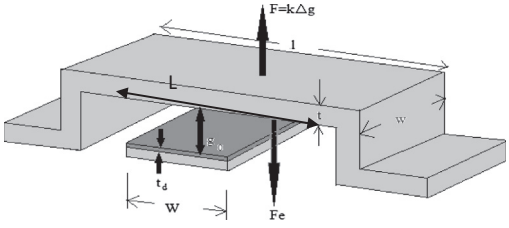

Figure 3 A MEMS switch with fixed–fixed beam.

Lakshminarayan et al. [19] have derived the formulae to calculate the value of up and down state capacitance with considering the two assumptions. The first assumption, while calculating up state capacitance 25% fringing field (P_f) was taken into account. Secondly, to calculate down state capacitance 54% dielectric roughness factor of isolation layer was considered. The expression for parallel plate capacitor (C_{pp}) of MEMS shunt switch is given by expression (2).

$$C_{pp} = \frac{\varepsilon_0 W w}{g_0 + \left(\frac{t_d}{\varepsilon_{rd}}\right)} \tag{2}$$

Therefore the up state capacitance and down state capacitance are given by Eqs. (3) and (4) respectively.

$$C_{up} = C_{pp}(1 + P_f) \tag{3}$$

$$C_{down} = (\varepsilon_0 \varepsilon_{eff} W w)/t_d \tag{4}$$

where $\varepsilon_{rd} = 6.8$ is the permittivity of silicon nitride, $\varepsilon_{reff} = 54\%$ of $\varepsilon_{rd} = 3.7$ and $P_f = 0.25$. The dimension of the designed MEMS switches is shown in Table 1.

By putting appropriate dimensions for Eqs. (2)–(4) we get capacitance values $C_{pp} = 0.986$ pF, $C_{up} = 1.23$ pF and $C_{down} = 18.78$pF respectively. The analytical value of capacitance ratio ($C_r = C_{down}/C_{up}$) = 15.27. Therefore from calcu-

Table 1 Dimension of the MEMS switches.

Parameters	L	l	w	W	t_d	t	g_0
Value (in mm)	1.46	2.08	0.2	0.86	0.0003	0.01	0.0015

lated value, it can be concluded that down state capacitance value increases by 15-fold compared to up state capacitance value.

3.2. Analysis of mechanical properties of MEMS switch

3.2.1. Calculation of spring constant (k) of MEMS switch

The spring constant of MEMS switch depends upon material properties of the switch such as Young's Modulus. The value of spring constant of non-meandered line is given by Eq. (5) [20].

$$k = \frac{32EWt^3}{L^3} \tag{5}$$

where, E, W, L and t are the Young's Modulus of gold (80 GPa), width of the beam, t thickness of beam, and length of beam where force is applied respectively. By putting values of all parameters of Eq. (5) from Table 1, the calculated spring constant is 164.52 N/m.

3.2.2. Calculation of the pull in voltage (V_{PI}) of MEMS switch

From the literature survey it has been shown that pull in effect [21] occurs when gap between the bridge and central signal line reduces to 2/3 of the original gap and the beam becomes unstable when gap exceeds 2/3 of the original. The value of pull in voltage required to go from up to down state expressed in Eq. (6).

$$V_{PI} = \sqrt{\frac{8kg_0^3}{27\varepsilon A}} \tag{6}$$

where $A = Ww$ = contact area and on calculation, the value of pull in voltage becomes with spring constant 164.52 N/m is 10.4 V.

3.2.3. Calculation of mechanical resonant frequency (f_0) of the MEMS switch

Chakraborty et al. [22] presented a formula to calculate the mechanical vibration of the beam has been written in Eq. (7).

$$f_0 = \frac{1}{2\pi}\sqrt{\frac{k}{m}} \tag{7}$$

where m is modal mass of the beam $= 0.35 \times (L \times w \times t) \times \delta$. The δ is density of gold $= 3.55 \times 10^{-13}$. By using values from Table 1, m = 19,320 kg/m^3 and on calculation the value of frequency of fundamental mode is 14.6 kHz.

3.2.4. Calculation of switching time (t_s) of each switch

An approximate time to perform complete up and down state of each beam is expressed by Eq. (8).

$$t_s = (3.67 \times V_{PI})/(V_s\omega_0) \tag{8}$$

where $V_s = 1.4V_{PI}$, ω_0 is the angular frequency of the switch. By analytical method, the switching time of each beam is 28.59 μs.

3.3. Analysis of electrical properties of MEMS switch

In addition to mechanical characteristic, we have to find out the electrical performance of MEMS switch. In MEMS switch: the spring acts as an inductor, the actuation voltage exhibits as a capacitor and the beam behaves as a resistance. The value of resistance (R), inductance (L) and capacitance (C) [23,24] is expressed in below:

$$R = \frac{\rho L}{tw} = \frac{L}{\sigma tw} \tag{9}$$

$$C = \frac{\varepsilon A}{g} \tag{10}$$

$$L = \frac{1000}{4\pi^2 Cf^2} \tag{11}$$

where ρ is the resistivity of gold, f is the resonant frequency in GHz and g is the gap between central line of CPW and beam, which will be varied. In our designed, the value of C and L changes, when the gap g has been reduced to acquire tunable characteristic. But, the resistance value is fixed and equal to 0.025 ohm.

4. Simulation result and discussion

The simulation of the designed antennas has been carried out in Ansoft HFSS v. 13 and different RF performance parameters of the antenna are also discussed in this section.

Fig. 4 depicts the plot between S11 parameters and frequency for the antenna in different states within frequency ranging from 13 GHz to 20 GHz. Simulation has been carried out at different states by activating 1, 2, 3 and 4 switches for both the up and down state respectively. At the time of simulation the initial gap of 1.5 μm has been chosen so that better capacitive can be achieved. But as reported in different literatures, the beam can snap down maximum up to 2/3 of initial gap and above this value beam becomes unstable. Hence, down state of the switches is considered as 1 μm. Fig. 4 demonstrates that the antenna covers many bands within frequency ranging from 13 GHz to 20 GHz at different states by activating 1, 2 3 and 4 switches. Tunable in resonant frequency has been obtained when switches moves from up do down state. The number of resonating band has been increased when the height of the bridges changes from 1.5 μm to 1 μm and S11 parameter moves more down for antenna with capacitive gap 1 μm with their respective state. The size of the device increases with

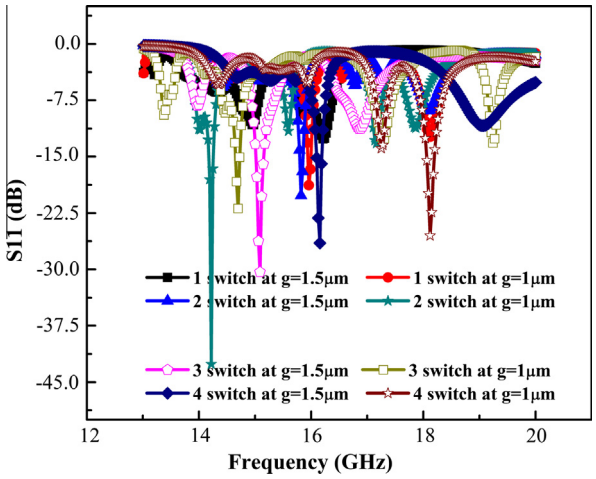

Figure 4 Simulated S11 parameters (dB) vs. frequency (GHz).

increase in number of switches. So proposed antenna can cover some different resonant frequencies within the frequency ranging from 13 GHz to 20 GHz. Hence the level of reconfigurability also increases by many folds.

Fig. 5 portrays the gain pattern of E-plane and H-plane for both the cases, antenna loaded with two switches ((a) and (b)) and four switches ((c) and (d)) at up and down state respectively. The simulation shows that gain pattern slightly distorted when the antenna is loaded four switches compared to the antenna loaded with two switches. When the switches move from up to down state, the gain pattern also changes. The back lobe gains of the antenna are unequal for E-plane and H-plane which occur at each state. But the amount of back lobe gain is more for antenna loaded with four switches in comparison with antenna loaded with two switches. Fig. 5 (a) and (b) shows that, for both E and H-planes the gain pattern is almost the same; hence, both E-plane and H-plane can be used as transmitting and receiving antenna.

Fig. 6 depicts the radiation pattern of the proposed device at up and down state in both E and H plane. Cross and Co

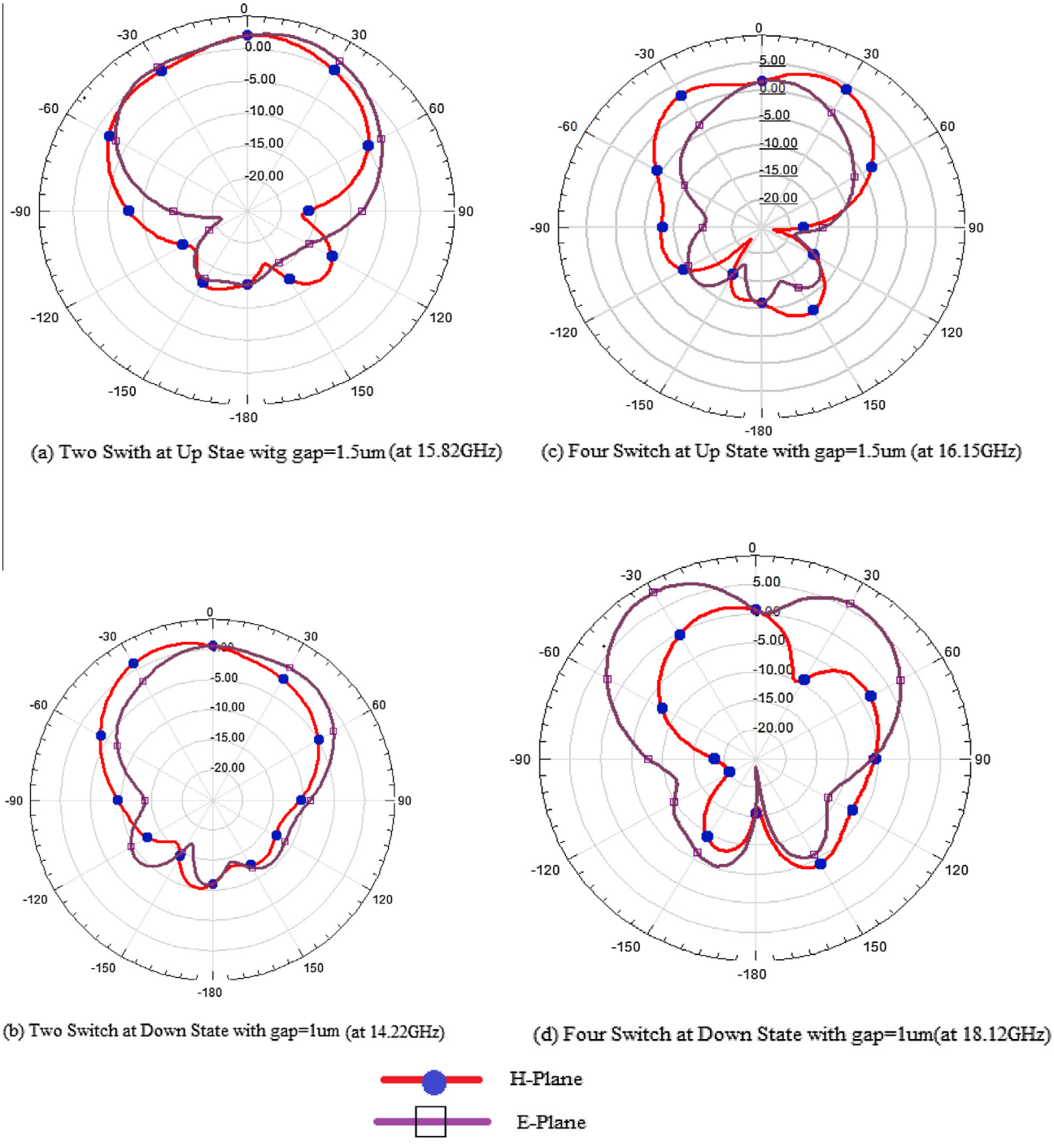

Figure 5 Simulated gain pattern of the antennas at H-plane and E-plane.

polarization has been indicated in the figure. Radiation pattern of the antenna depends on the radiation resistance but radiation resistance varies from structure to structure. Radiation pattern of cross and co polarization also changes when switches move from up to down state for both E and H planes. Radiation pattern shown in Fig. 6(b) and (d), shows better performance as the level of cross-polar is less than the level co-polar and hence no loss will occur. But for other two cases due to presence of higher order modes, level of radiation pattern of cross-polarization polarization crosses the co-polarization within some beamwidth as shown in Fig. 6 (a) and (d). But, for remaining beamwidth level of cross polarization is less than co-polarization.

Fig. 7 illustrates the simulated efficiency of the antennas for antenna loaded with two and four switches. High efficiency has been obtained at their corresponding up and down state in both cases and either the antenna geometry is loaded with two or four switches. Table 2 depicts the comparison in performance at different states of the switches.

5. Parametric analysis of MEMS switches and CSRRs

5.1. Parametric analysis of MEMS switch

This section includes effects in electrical characteristic due to various dimensions of MEMS switches. Effects in S11 parameter due to change in dimension of beam width, beam thickness, and air gap height are elaborately discussed.

5.1.1. Effect of beam width

A parametric analysis has been done by varying bridge width for both up and down states with beam thickness (t) = 10 μm is shown in Figs. 8 and 9 respectively. The resonance frequency is varied when bridge width is varied and variation is more for

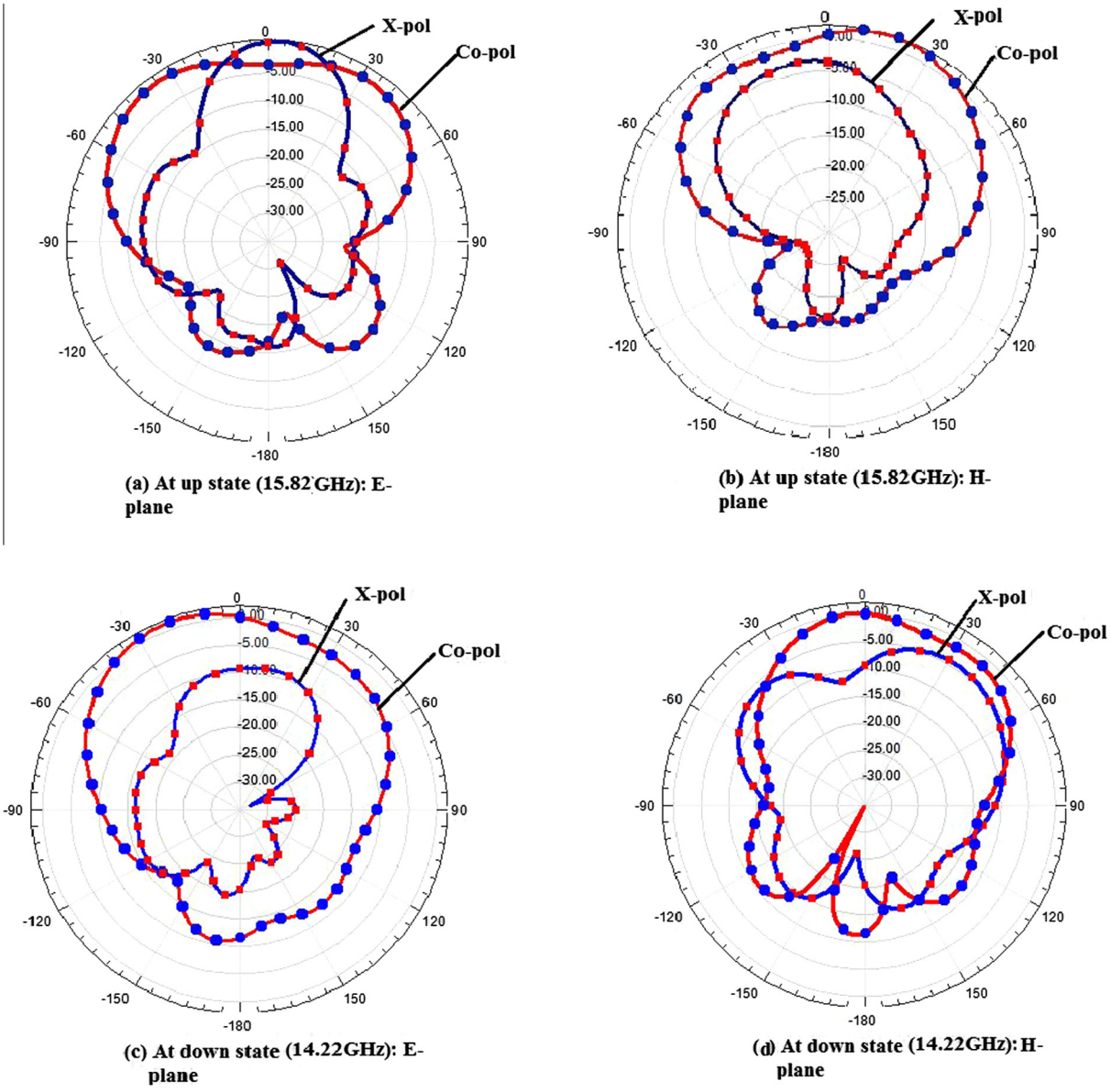

Figure 6 Radiation pattern of the antenna at different states in E-plane and H-plane.

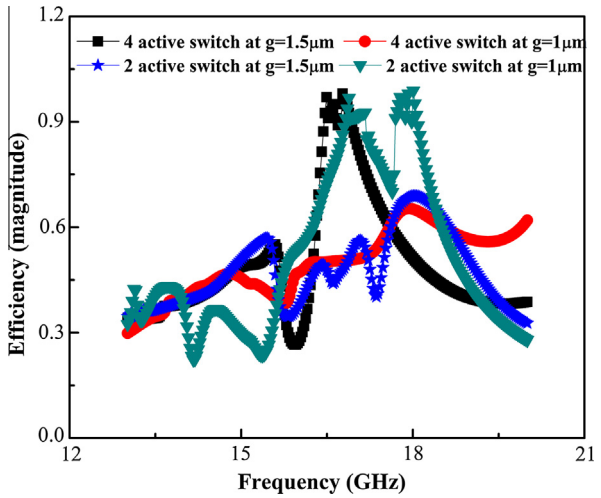

Figure 7 Simulated efficiency (magnitude) vs. frequency (GHz).

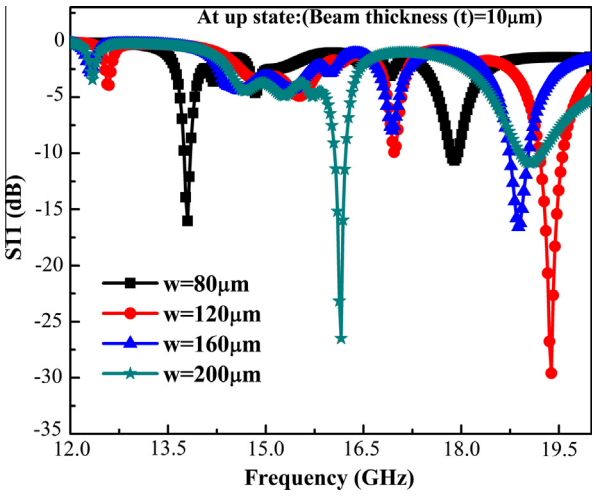

Figure 8 Parametric analysis of bridge width corresponding to the up state (g = 1.5 μm) and beam thickness t = 10 μm.

down state; S11 value falls more down at down state of the switches. This is due to down state both inductive and capacitive effect will be there, while at up state only capacitive effect is present [25]. At w = 200 μm, at down and up state (fr, S11) are (18.12 GHz, −25.52 dB) and (16.15 GHz, −26.5 dB) respectively. S11 value is more down for w = 120 μm. In our design, we have considered w = 200 μm as it can afford actuation mechanism more efficiently and also shows better performance at up as well as down state.

5.1.2. *Effect of beam thickness*

Parametric analysis of bridge thickness while keeping all other parameters constant at up and down state is portrayed in Figs. 10 and 11 respectively. Down state shows better performance in terms of S11 compared to up state. Again from Eq. (6), with increase in beam thickness t, spring constant k increases and results in increase in pull-in voltage. At t = 6 μm, for up state s-parameter does not show better performance. An optimum performance has been obtained both for up and down states at beam thickness (t) = 10 μm. Hence, in our proposed device we have considered thickness of beam (t) = 10 μm.

5.1.3. *Effect of air–gap height*

Fig. 12 depicts the parametric analysis of the proposed device different between the central line of CPW and the beam. At different air–gap, S11 value with their corresponding resonant

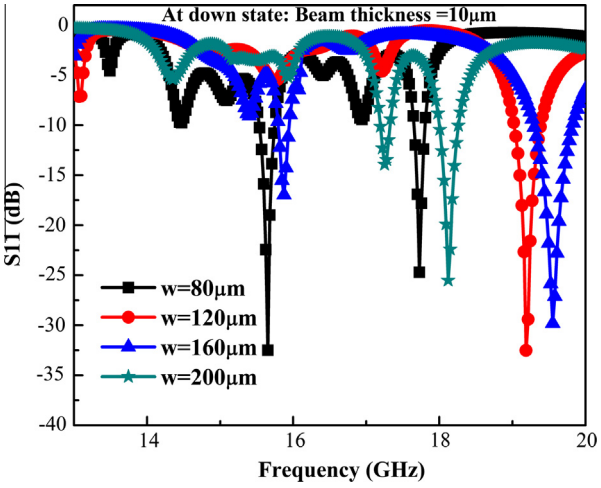

Figure 9 Parametric analysis of bridge width corresponding to the down state (g = 1 μm) and beam thickness t = 10 μm.

frequency also changes. But switch is stable up to 2/3 of the initial gap and above this it becomes unstable. Hence we have shown parametric analysis from initial gap of 1.5 μm to critical gap up to 1 μm. At these two gaps antenna performs very well in terms of S11-parameters.

Table 2 Comparison of tunable performance at different states.

State	Resonance frequency (GHz)	S11 (dB)	Shift in frequency (GHz)
1 switch at g = 1.5 μm	16.24	−12.55	0.28
1 switch at g = 1 μm	15.96	−18.81	
2 switch with g = 1.5 μm	15.82	−20.17	1.6
2 switch with g = 1 μm	14.22	−42.61	
3 switch with g = 1.5 μm	15.09	−30.35	0.4
3 switch with g = 1 μm	14.69	−21.92	
4 switch with g = 1.5 μm	16.15	−26.49	1.97
4 switch with g = 1 μm	18.12	−25.52	

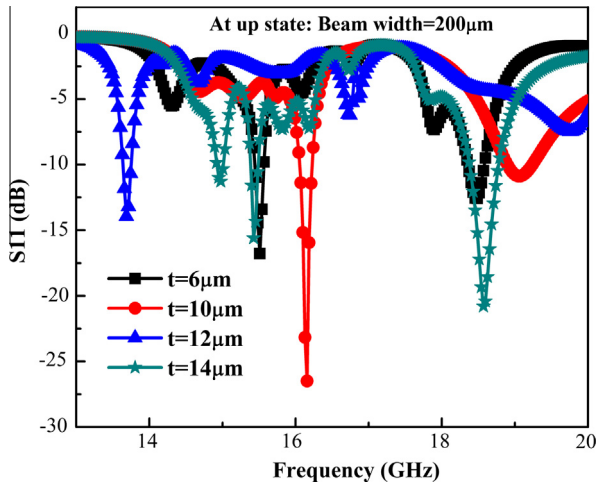

Figure 10 Parametric analysis of bridge thickness corresponding to the up state (g = 1.5 μm) and beam width = 200 μm.

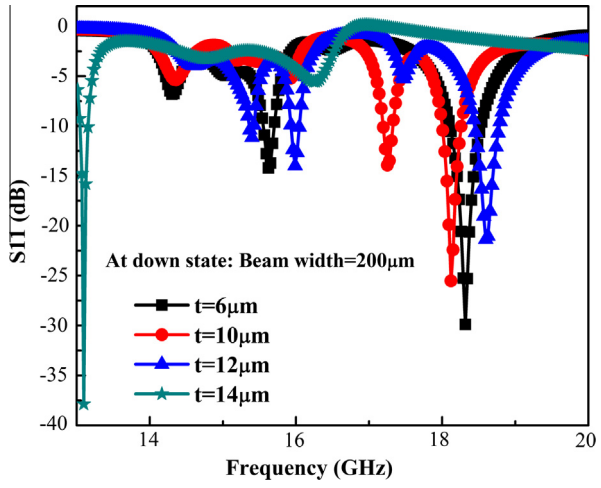

Figure 11 Parametric analysis of bridge thickness corresponding to the down state (g = 1 μm) and beam width = 200 μm.

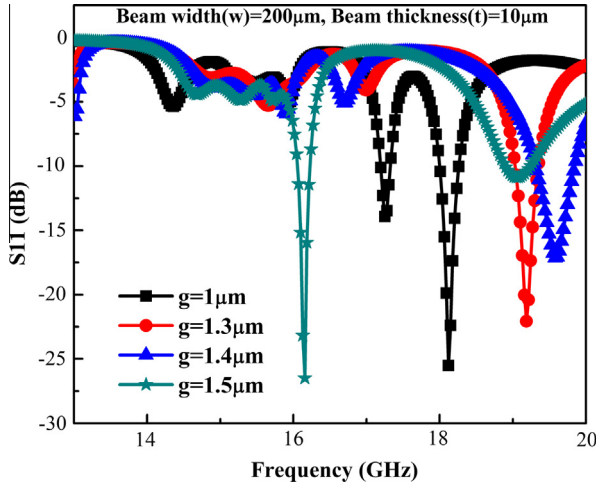

Figure 12 Parametric analysis of air gap height (g) at fixed beam width (w) = 200 μm and beam thickness (t) = 10 μm.

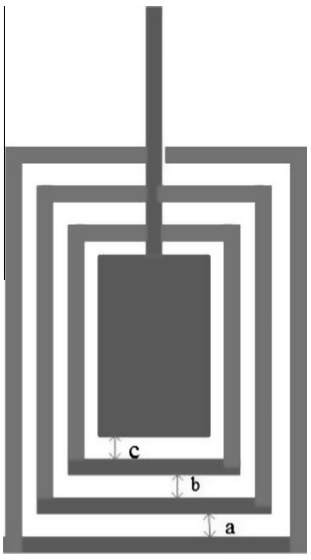

Figure 13 A part CSSRs to show different radius.

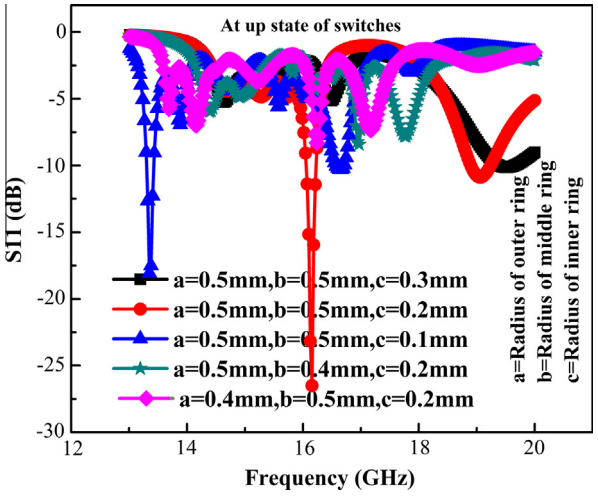

Figure 14 Parametric analysis of CSRRs by varying the radius of ring corresponding to the up state (g = 1.5 μm).

5.2. Parametric analysis of CSRRs

In this section parametric analysis of CSRRs by varying the radius of the ring and fixing other parameters was carried out. Fig. 13 portrays the top view of CSRRs, where a, b and c are outer, middle and inner ring radius respectively.

Figs. 14 and 15 depict the parametric analysis of CSRRs by varying the radius of the ring (a, b and c) while fixing the other dimension. At up state antenna radiates only for two combinations 0.5 mm × 0.5 mm × 0.2 mm and 0.5 mm × 0.5 mm × 0.1 mm; it does not have any radiating band for other three combinations. On the other hand, at down state antenna radiates for all combinations of radius. But for combination 0.5 mm × 0.5 mm × 0.2 mm, a reasonable S11 value has obtained both at up (S11 = -26.5 dB) and down states (S11 = −25.52 dB). Hence, CSRRs with radius 0.5 mm × 0.5 mm × 0.2 mm is favorable.

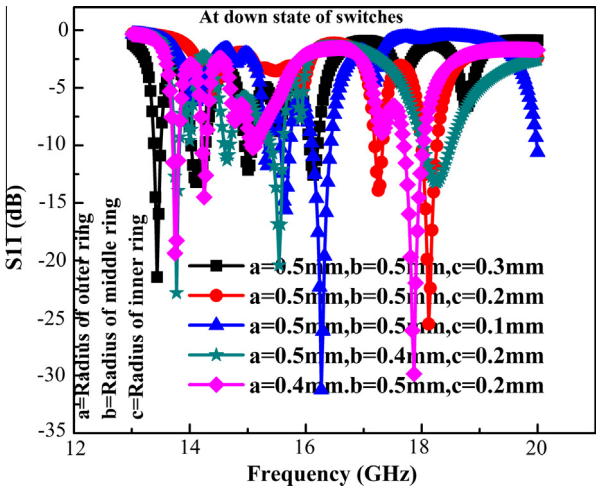

Figure 15 Parametric analysis of CSRRs by varying the radius of ring corresponding to the down state (g = 1 μm).

6. Conclusion

This work shows the design and simulation of a tunable antenna which is loaded with CPW stub on which MEMS switches are placed. The antenna has been implemented on silicon substrate with an air cavity between the patch and ground; and uses monolithically integration of MEMS switches to achieve tunable performance. The dimensions of the CPW ground are made larger in order to obtain proper transition of signal between the CPW ground and ground plane of patch antenna. When antenna moves from up to down state loaded with one, two, three and four switches provide frequency shift of 0.28 GHz, 1.6 GHz, 0.4 GHz and 1.97 GHz respectively. This work demonstrated that tunable in resonant frequency, bandwidth and radiation pattern by changing the capacitive gap and level of reconfiguration enhanced by increasing the number of switches. The comparison of tunable performance for up and down condition of the switches at different state is shown in Table 2. This paper comprises the mechanical and electrical performance of MEMS switch. The analytical value of actuation voltage is very low of about 10.4 V. The capacitance ratio is also shown better performance having value of 15.27. In order to show sensitivity of the antenna, a parametric analysis of MEMS switch and CSRRs has been presented.

Acknowledgment

The authors would like to convey their thanks to Jadavpur University for providing software facility on carrying out this work.

References

[1] Ali Pourziad, Saeid Nikmehr, Hadi Veladi, A novel multistate integrated RF MEMS switch for reconfigurable antennas applications, Prog. Electromagn. Res. 139 (2013) 389–406.
[2] G.M. Rebeix, RF MEMS Theory, Design and Technology, Wiley, Hoboken, NJ, 2003.
[3] J.K. Smith, Reconfigurable Aperture Antenna (RECAP), DARPA, 1999 (online). Available: <www.darpa.mil>.
[4] D. Mercier, K.V. Caekenberghe, G.M. Rebeiz, Miniature RE MEMS switched capacitors, in: Proceedings of the IEEE MTT-S Digest, 2005, pp. 745–748.
[5] S. Nikolaou, N.D. Kingsley, G.E. Ponchak, J. Papapolymerou, M.M. Tentzeris, UWB elliptical monopoles with a reconfigurable band notch using MEMS switches actuated without bias lines, IEEE Trans. Antennas Propag. 57 (8) (2009) 2242–2251.
[6] R.N. Simons, D. Chun, L.P.B. Katehi, Microelectromechanical systems (MEMS) actuator for antenna reconfigurability, in: IEEE MTT-S Int. Microwave Symp. Digest, May 2001, pp. 215–218.
[7] Emre Erdil, Kagan Topali, Mehmet Unlu, Ozlem Aydin Civi, Tayfun Akin, Frequency tunable microstrip patch antenna using RF MEMS technology, IEEE Trans. Antennas Propag. 55 (4) (2007) 1193–1196.
[8] Christos G. Christodoulou, Youssef Tawk, Steven A. Lane, Scott R. Erwin, Reconfigurable antennas for wireless and space applications, Proc. IEEE 100 (7) (2012) 2250–2261.
[9] Nickolas Kingsley, Dimitrious E. Anagnostou, Manos Tentzeris, John Papapolymerou, RF MEMS sequentially reconfigurable sierpinski antenna on a flexible organic substrate with novel DC-biasing technique, J. Microelectromech. Syst. 16 (5) (2007) 1185–1192.
[10] Constantine A. Balanis, Modern Antenna Handbook, A John Wiley & Sons, 2008.
[11] Linda P.B. Katehi, James F. Harvey, Elliott Brown, MEMS and Si micromachined circuits for high frequency applications, IEEE Trans. Microw. Theory Tech. 50 (3) (2002) 858–866.
[12] Erik Öjefors, Micromachined Antennas for Integration with Silicon Based Active Devices, Uppsala University, 2004.
[13] Ioannis Papapolymerou, Rhonda Franklin Drayton, Micromachined patch antennas, IEEE Trans. Antennas Propag. 46 (2) (1998).
[14] Poonam Verma, Surjeet Singh, Design and simulation of RF MEMS capacitive type shunt switch & its major applications, IOSR J. Electron. Commun. Eng. (IOSR-JECE) 4 (5) (2013) 60–68, e-ISSN: 2278-2834, p-ISSN: 2278-8735.
[15] K. Topalli, M. Unlu, H.I. Atasoy, O.A. Civi, S. Demir, T. Akin, Empirical formulation of bridge inductance in inductively tuned RF MEMS shunt switches, Prog. Electromagn. Res., PIER 97 (2009) 343–356.
[16] Chnag won Jung, Ming-jer Lee, G.P. Li, Franco De Flaviis, Reconfigurable scan-beam single-arm spiral antenna integrated with RF-MEMS switches, IEEE Trans. Antennas Propag. 54 (2) (2006) 455–463.
[17] Deng Zhong Liang, Wang Hui Jun, A design of antenna with pattern reconfigurable characteristic working on Ka band, in: Proceedings of 2012 International Conference on Mechanical Engineering and Material Science (MEMS), 2012, pp. 720–723.
[18] Ozlem Aydın Civi, Simsek Demir, Tayfun Akin, Reconfigurable Antennas Using RF-MEMS Research in Turkey, IEEE, 2011, 978-1-61284-757-3/11/$ 26.00 C2011.
[19] B. Lakshminarayan, D. Mercier, G.M. Rebeiz, High reliability miniature RF MEMS switched capacitors, IEEE Trans. Microw. Theory Tech. 56 (2008) 971–981.
[20] J. Gere, Mechanics of Materials, fifth ed., Thompson-Engineering, 2003.
[21] S. Senturia, Microsystem Design, Kluwer Academic Publishers, 2001.
[22] Amrita Chakraborty, Bhaskar Gupta, Binay Kumar Sarkar, Design, fabrication and characterization of miniature RF MEMS switched capacitor based phase shifter, Microelectron. J. 45 (2014) 1093–1102.
[23] D. Pozar, Microwave Engineering, second ed., John Wiley and Sons, Inc, New York, NY, 2001.

[24] Sandeep Chaturvedi, G. Sai Saravanan, Madhav K. Bhat, Sangam Bhalke, S.L. Bandikar, R. Muralidharan, Shiban K. Koul, Design and electrical characterization of wafer-level micro-package for GaAs-based RF-MEMS switches, IETE J. Res. 59 (2013) 201–209.

[25] Ngasepam Monica Devi, Santanu Maity, Rajesh Saha, Sanjeev Kumar Metya, in: RF MEMS and CSRRs-based tunable filter designed for Ku and K bands application, Cogent Eng., vol. 2, Taylor and Francis, 2015, pp. 1–14.